Global Flow Measurement Workshop
25 - 27 October 2022

Technical Paper

Metering and emission analysis of flare and vent metering systems using Computational Fluid Dynamics

Sandy Black, TÜV SÜD National Engineering Laboratory
Marc Laing, TÜV SÜD National Engineering Laboratory
David Newman, bp

1 INTRODUCTION

Flaring and venting are contributors to greenhouse gas emissions and have been estimated to account for more than 500 million tonnes of carbon-dioxide equivalent emissions in 2020, which is more annual CO_2 emissions than from all the cars in the European Union [1]. However, flaring and venting are both critical safety components of any oil and gas producing facility, allowing for the safe disposal of unplanned or excess gases which cannot be safely processed. Flare and vent gas is comprised of a mix of methane and other hydrocarbons which can be vented or flared by converting the gas to carbon dioxide through combustion.

Methane is understood to have a shorter atmospheric lifetime but a much higher global warming potential than carbon dioxide and therefore, paradoxically, flaring any methane emissions that would otherwise reach the atmosphere reduces the environmental impact of hydrocarbon production.

Accurate flare and vent gas metering is important to report the correct quantities of methane flowing to the vents and / or flares. This is important to meet regulatory requirements, but to also ensure that the flare systems are sufficiently purged to prevent the formation of combustible mixtures within the stack resulting in flashback or burn-back issues. Furthermore, an incorrect meter reading could also lead to sub-optimal operation of the flare system and lead to higher quantities of greenhouse gases being released into the atmosphere.

Therefore, flaring and venting systems must be accurately measured, operate above their mimimum safety flow rate and in the case of flaring achieve a high combustion and destruction efficiency to reduce emissions. In the case of venting, a reduction in emissions can be achieved by reducing the flow rate of gas leaving the vent. However, operating these systems at such low levels maybe significantly out-with their original design specification. Additionally, in the case of flaring, the combustion efficiency can be inherently linked to meterological conditions such as the wind which dilutes and cools the combustion zone.

To address these issues, TÜV SÜD National Engineering Laboratory (NEL) have been working with bp to perform Computational Fluid Dynamics (CFD) modelling on their global production flare and vent systems, with the aim of understanding, verifying and ultimately reducing bp's overall methane intensity in a safe and efficient manner from all of bp's global upstream production assets. This is part of bp's Aim 4 plans which supports delivering bp's net zero ambition.

This paper demonstrates this approach as a valuable method to increase flaring and venting knowledge of existing assets and can help significantly reduce the impact on the environment from flaring and venting.

2 METHODOLOGY

The CFD simulations are focussed on two main areas:

- Ultrasonic and thermal mass meter correction for flare and vent systems
- Flare tip combustion and destruction removal efficiency analysis.

Both areas are used to evaluate how efficiently the flare system is operating and how efficient the flare systems are in reducing the greenhouse gases being emitted.

The ultrasonic and thermal mass flare and vent meter correction is focussed on ensuring that even in a non-ideal installation the flow meter provides accurate flare and vent gas flow rates. This is done by calculating the flow rate of the flare or vent meter that would be measured in situ and then deriving an appropriate k-factor (correction factor) to correct the output of the flare / vent meter across its operating range.

For the combustion and destruction removal efficiency analysis, a 3D model of the flare tip is generated and different process conditions are modelled using CFD with a detailed combustion chemistry mechanism. The model accounts for different external influences such as humidity, wind speed and wind direction along with the flare gas flow rate, gas composition, temperature and other equipment such as ignitors or flare assist mechanisms and the effects of co-located flares (i.e. multiple flares operating in close proximity). The analysis is primarily used to determine the combustion efficiency (CE) and the destruction & removal efficiency of methane (DRE). However it has also been used to evaluate other observations of the flare tip such as flashback potential and areas that could succumb to thermal fatigue.

The two areas are intrinsically linked as the meter correction analysis is important to first understand the flow rate entering the flare tip. These two parameters are key to determining how efficiently the flare system is operating and the quantity of greenhouse gases being emitted.

3 FLARE METER ANALYSIS

Flares are necessary to quickly dispose of hydrocarbon gas in emergencies, however these release greenhouse gas emissions such as carbon dioxide (CO_2) and methane (CH_4). Currently, CO_2 emissions are strictly regulated, such as under the EU Emissions Trading Scheme (ETS) or the U.S. Environmental Protection Agency (EPA) which places limits on the amount of CO_2 emissions operators can release year on year, however, it is expected in the near future that CH_4 will follow similar regulation. Producers are therefore required to measure the amount of CO_2 released by flares within certain accuracies, and ensure the amount released stays within their emissions quotas.

3.1 Flare gas measurement

The measurement of flare gas is difficult as the range of flow rates to be metered requires a large turndown ratio, from a minimum purge rate to prevent any air ingress back into the system to a full blowdown. As a consequence of this, flare gas lines can be over 60 inches in diameter. The measurement should also have minimal pressure drop and require a low level of maintenence as these will often be installed in areas that are difficult to remove and would require significant downtime for the asset.

The most widely used measurement techology is Ultrasonic Flow Meters (UFMs). This technology allows a high turndown ratio, can be installed in large diameter pipework, has minimal pressure drop and the meters can be serviced without any downtime and removal of the meter.

A schematic of a typical single path ultrasonic flow meter is shown in Figure 1. The transit time from transducer 1 to transducer 2 (T_{12}) is first measured travelling with the flow. Then the transit time from transducer 2 to transducer 1 (T_{21}) is measured travelling against the flow. The transit time travelling with the flow will be shorter than the time travelling against the flow and will be proportional to the velocity of the gas at the point of measurement.

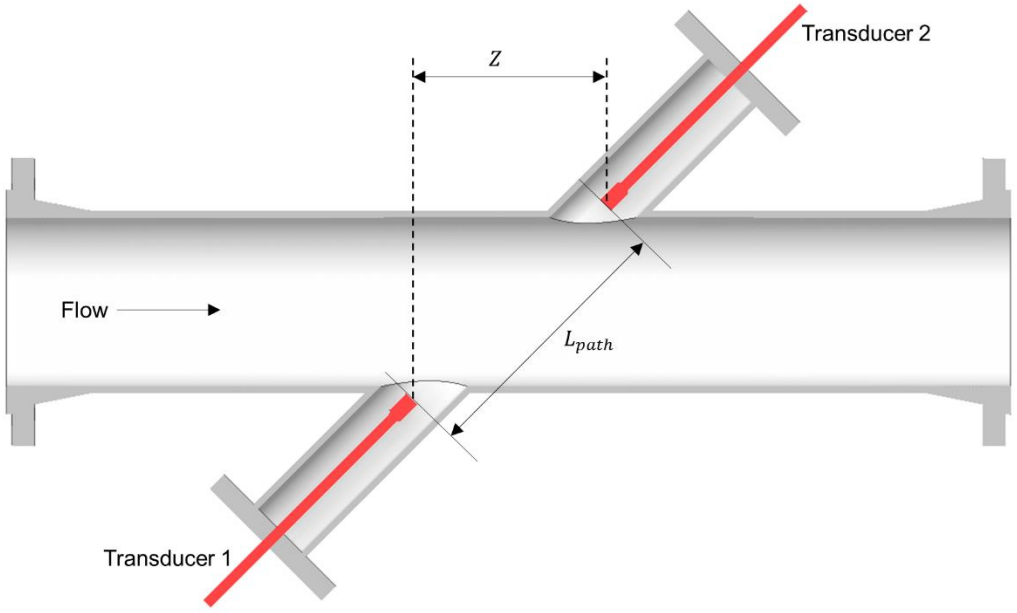

Fig. 1 Ultrasonic flow meter schematic

To determine the gas velocity of an individual path, V_{path}, in the pipe, the following equation can be used

$$V_{path} = \frac{L_{path}^2}{2Z}\left(\frac{T_{21} - T_{12}}{T_{21} \cdot T_{12}}\right) \quad (1)$$

where L_{path} is the path length between the two transducers and Z is the lateral distance along the pipe axis and in the flowing gas between the two transducers. To determine the volumetric flow rate, the the cross-sectional area of the pipe can be multiplied by mean velocity $\bar{V}$. Different manufacturers may have different methodologies for computing this average if multiple transducers are used.

Whilst this approach may seem simple, the calculation of the flow rate requires an ideal flow profile and the actual location of the transducers may also require a further correction. For example, in some applications the measurement is only

taken in part of the flow profile and a correction factor K, or k-factor, is also requried.

Furthermore, in flare gas metering applications an ideal flow profile is rarely achieved as upstream components such as bends, tee pieces, thermowells, branches and any other intrusive items cause flow distrubances. A rule of thumb amongst meter manufactuers is to have at least 20 straight pipe diameters upstream of the meter and 5-10 straight pipe diameters downstream [2]. However, in most installations this is not practically possible. The meter is designed and assumed to work with an ideal undisturbed flow however depending on the position of the meter and any upstream pipework, the gas velocity of the individual path can be different. Figure 2 shows an example of the difference between the path velocity in an ideal situation and one with a flow disturbance, often referred to as installation effects. The average path velocity in the ideal situation is 20.48 m/s whereas in the installed configuration the average velocity is 19.77 m/s resulting in a 3.5 % bias error. Therefore, the k-factor installed within the meter may not be sufficient.

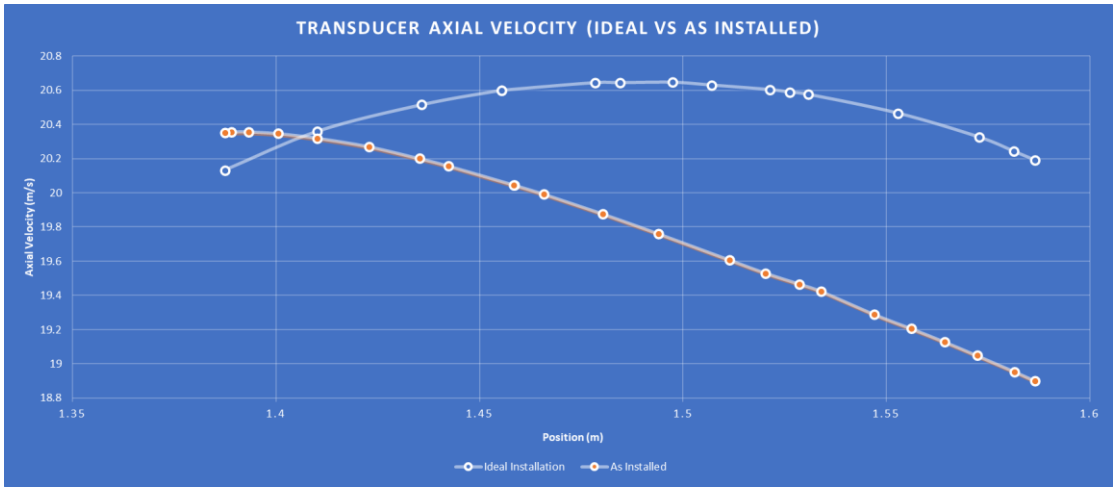

Fig. 2 Path velocity showning an example of an ideal and a distrubed flow profile.

Installation effects are difficult to recreate in calibration laboratories because of a number of factors. Flare gas meters are often installed in areas where they are difficult to remove, often requiring secondary structures to be built and significant downtime for the asset which is obviously undesirable. Flare gas meters are often welded into the line, making removing them difficult. At present, there are no facilities available to calibrate the full flow range of flare gas meters because in extreme cases meters can be up to 60 inch diameter flowing at up to 150 m/s. Furthermore, if a facility could replicate the flow rates it would not be practically possible to calibrate the meter in the exact installation due to the size and scale of the installation. The reality is that the only practical way to correct the flare gas meter in situ is to use CFD to determine appropriate k-factors across the full design envelope of the facility.

3.2 The use of CFD analysis

The use of CFD models has and will be used to determine the k-factors of each of bp's flare and vent lines worldwide. The following steps are performed when determining the appropiate k-factors:

- A full 3D model of the wetted volume of the flare line is generated either from a 3D CAD model or isometric drawings. If available, this will include the model of the transducers within the meter. An example is shown in Figures 3 and 4.
- A total of 10 flow points are modelled which account for the full design envelope of the meter.
- The modelled flow rate from CFD is then compared to an uncorrected predicted flow rate that a UFM would output in this scenario. Therefore, if the predicted flow rate is higher than the modelled flow rate the meter would be 'over reading'.
- A range of k-factors are then derived and given as a function of transducer Reynolds number.

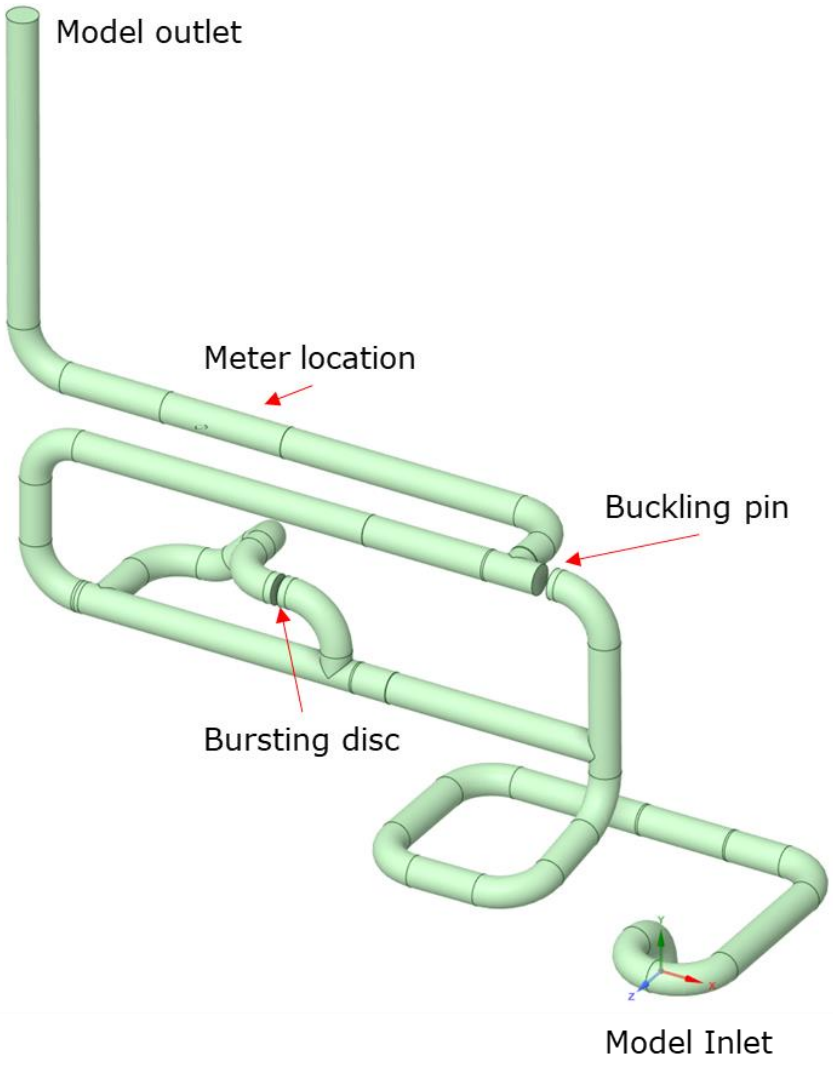

Fig. 3 An example a flare metering installation.

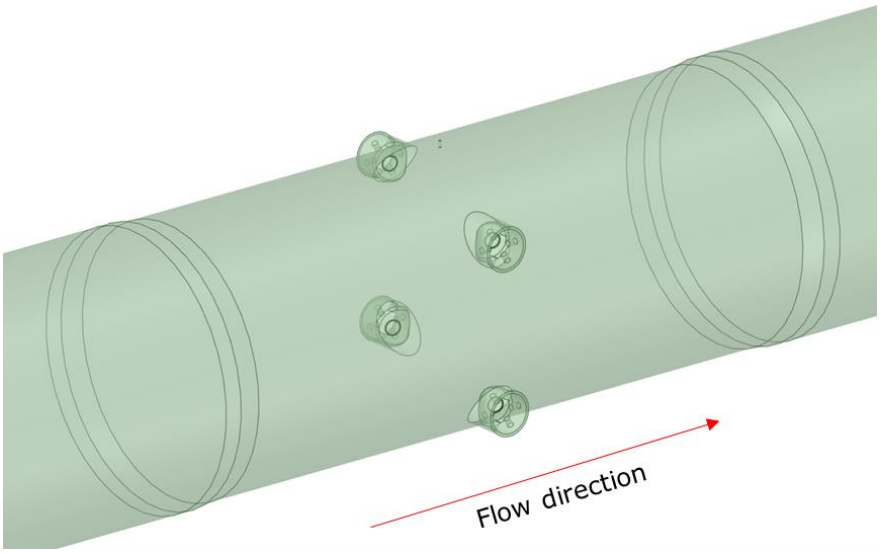

Fig. 4 An example of a dual path meter geometry used in the CFD analysis.

The CFD models are performed using the commerical CFD software, ANSYS Fluent, and are generated using high quality polyhedral meshes with sufficient refinement at the wall boundary to resolve the viscous sublayer.

The flow is assumed to be steady and incompressible, the realisable k-ϵ turbulence model was used in most cases and second order discretisation schemes are used for most of the equations.

A constant mass flow boundary condition is used at the inlet to the model, the walls are set as no slip boundary condition and a pressure outlet is set at the outlet of the models. The predicted meter velocity and pressure drop in the CFD simulations are used as criteria to ensure the simulations are converged.

The model size can vary between 4 million to 150 million cells depending on the complexity, length and size of the models. Grid independence is assessed where reasonably possible and most meshes tend to be independent in the order of 50 million cells. The simulations are computed on TÜV SÜD National Engineering Laboratory's internal high performance computing (HPC) cluster on up to 640 cores.

The location of the UFM transducers and their position are either determined from a combination of the CAD drawings, GA drawings, meter config files and pictures of the installation. On occasion, pictures of the installation have shown key differences such as the meter being installed backward which can then be included in the analysis. This information is then used to extract the gas velocity of the actual path from the CFD analysis and converted into a predicted flow rate $Q_{predicted}$. A single k-factor can be calculated as the ratio between the predicted flow rate and the actual flow rate that was supplied to the inlet to the CFD model, Q_{actual}:

$$k_{CFD} = \frac{Q_{actual}}{Q_{predicted}} \quad (2)$$

The absolute error can also be reported as

$$Absolute\ Error\ (\%) = 100 \times \frac{Q_{predicted} - Q_{actual}}{Q_{actual}} \quad (3)$$

An example of the typical output from the CFD analysis is given in Table 1. As is shown in the table, the meter would typically over-read the actual flow rate and requires a k-factor less than 1 to provide the correct meter reading. Furthermore, the k-factor is not constant for different flow rates and in this example there is a clear difference at the lower flow rates compared to the higher flow rates.

Table 1 – Example of output from CFD analysis

Case	Actual Flare System Flow rate (m^3/s)	Predicted Flare Flow rate from CFD (m^3/s)	Abs. Error (%)	Pipe Reynolds Number	Transducer Reynolds Number	k-factor
1	0.860	0.967	12.431	770,245	267,224	0.889
2	1.720	1.908	10.940	1,540,490	527,361	0.901
3	2.579	2.810	8.937	2,310,736	776,756	0.918
4	3.439	3.709	7.844	3,080,981	1,025,286	0.927
5	8.598	9.207	7.084	7,702,452	2,545,164	0.934
6	13.757	14.648	6.477	12,323,924	4,049,167	0.939
7	18.915	20.070	6.102	16,945,395	5,547,975	0.942
8	24.074	25.476	5.823	21,566,867	7,042,499	0.945
9	29.233	30.884	5.647	26,188,338	8,537,398	0.947
10	34.392	36.309	5.577	30,809,809	10,037,323	0.947

There are a number of ways the k-factor from Table 1 can be implemented into an ultrasonic meter:

- **A constant value**
  A single value applied over the entire flow range
- **Tabulated values**
  This can either be a function of velocity, or a function of Reynolds number.

A constant value would either choose a value from the table or be an average of all of the values and this would be applied regardless of flow rate. Alternatively, a tabulated approach which considers how the k-factor changes with flow rate could be used. Some meter manufacturers allow this table to be applied directly to the flow computer, however this could also be calculated externally from uncorrected flow velocity values. However, careful attention is required to determine the steps in which the meter applies the k-factor. For example, if any internal post-processing of the flow rates is performed this needs to be removed or cancelled out before this approach can be used.

A tabulated approach would be considered to be more accurate since the k-factor is sensitive to the flow profile. Figure 5 shows the impact of a tabulated approach of velocity and for Reynolds number for different gas densities of a typical mid-radius metering installation. If the density is unknown, this could lead to a higher

level of uncertainty in the k-factor at a particular flow velocity. This highlights that the use of Reynolds number would be preferable as the density of the gas can change throughout the flow range. For example the line pressure and temperature at purge conditions will be different from a blow-down scenerio resulting in different densities. Additionally, the composition of the gas can change depending on the scenerio, for example the flare gas might be diluted with nitrogen under purge conditions or contain heavier hydrocarbons during blow-down conditions which would also result in different densities.

In some flare gas meters, the flare gas density can be inferred through the use of proprietary algorithms that infer the density through the measurement of the speed of sound, pressure and temperature. To further improve the measurement, bp are installing flare gas analysers plus a gas chromatograph on the majority of their flare gas metering lines. This allows for an improved measurement of the flare gas composition, calculation of the density and dynamic viscosity (or alternatively kinematic viscosity) and therefore allows the Transducer Reynolds number k-factors to be used with the ultrasonic meter.

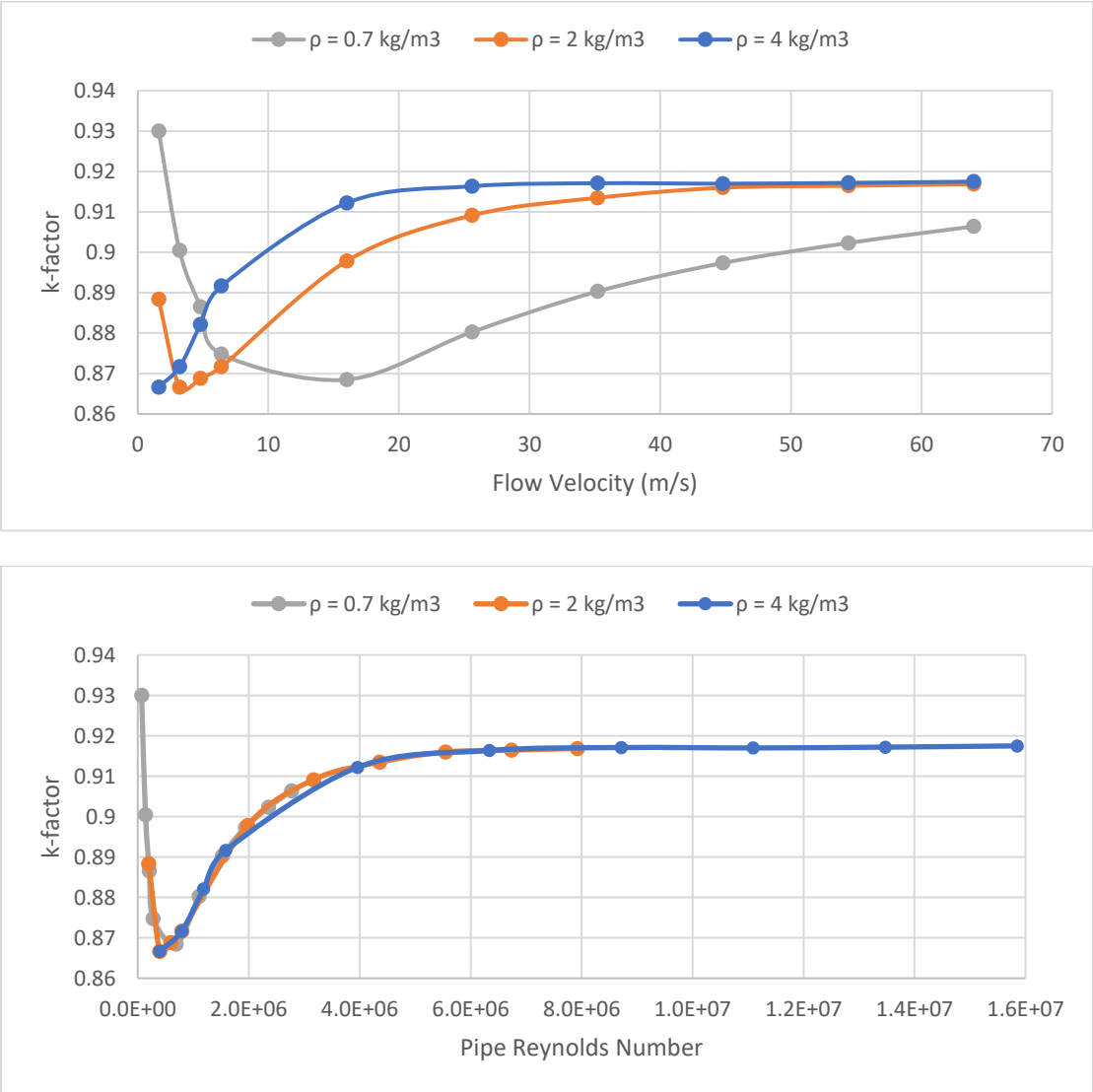

Fig. 5 An example k-factors based on pipe velocity and then Reynolds number

The k-factor would be installed after the measurement of the transit time or meter velocity. Therefore, the pipe Reynolds number or pipe velocity is not known before a k-factor is applied and the transducer Reynolds Number should be used. The transducer Reynolds number is calculated across the transducer path:

$$Re = \frac{\rho \cdot V_{path} \cdot L_{path}}{\mu} \quad (4)$$

where ρ is the density of the fluid [kg m^{-3}], μ dynamic viscosity of the fluid [Pa·s], V_{path} is the axial velocity taken across the path [m s^{-1}] and L_{path} is the path length of the transducer [m].

3.3 Lessons learned

The meters on bp's flare systems are ultrasonic flare gas meters. To date, 17 flare meters are single path mid-raidus, 24 are single path diameter, 12 are dual path mid-radius, 10 are dual path diametric with the remaining meters consisting of dual path crossduct and elbow meters. Around 90 % of the meters are installed either horizontally or on an inclined boom with the other 10 % being installed vertically.

Across all of the assets there is a large spread in k-factors from 0.8 to 1.4 and there is no noticable trend based on upstream / downstream length requirements or meter type highlighting that these meters are nominally always subject to some form of installation effect.

The work to date has confirmed that ultrasonic flare meters correction factors are a function of meter Reynolds number and highlights the importance of knowledge of the density and viscosity of the flare gas to compute the Reynolds number. In most installations around the world, the density and viscosity of flare gas is not continuously monitored and could lead to a high uncertainty in the meter correction factor that is applied.

Regardless of meter, it was typically shown that the measurement error is greater at lower Reynolds numbers and tends to flatten towards the top of the flow range. The meter traditionally operates at the low end and therefore such a correction is important so that unnecessarily high reported methane emissions are prevented. In most simulations, the meter was found to be over-reading and over-reporting the flow rate.

Operating at the lower end is important because the manufacturer of the flare tip provides a minimum purge rate which must be maintained to prevent atmospheric ingress to the tip and prevent potential internal combustion and flashback. If the meter is over reading and the process is set to maintain the minimum purge (which is often the case), then the flare is actually being operated below the minimum purge and this is potentially a serious safety issue. Additionally, the operator is reporting higher CO_2 and methane emissions. However, flowing gas at a lower rate than the minimum purge can reduce the overall efficiency of the flare therefore resulting in poorer combustion and greater greenhouse gas emissions to the environment.

4 FLARE TIP ANALYSIS

Flaring plays a critical role in process safety during the production of hydrocarbons both offshore and onshore, and during refinery operations. Flare tips are designed to allow the safe disposal of the excess or unplanned hydrocarbon release. Methane is typically the most prominent hydrocarbon compound found in flare gas however it has a more potent greenhouse gas effect than carbon dioxide. Therefore, flare systems typically have a pilot for ignition system that ignites the flare gas and converts methane to CO_2 to reduce its environmental impact.

Most flares are designed such that they operate on an elevated flare stack or an angled boom and can be over 50 m in length which is normally dictated based on the radiant heat intensity generated by the flare. The flare tip designs vary based on being connected to a high pressure or low pressure system, flow rates, temperature, location, gas composition and the environment. The flare design can include smoke suppression assist systems such as air or steam assist, typical for onshore installations or are non-assisted which is typical for an offshore installation. Additionally, the tip design can include multiple outlets / arms, fixed area or variable area sonic or Coandă nozzles, stabilisation tabs, windshields and ignitors. An example of an HP and LP tip is shown in Figure 6.

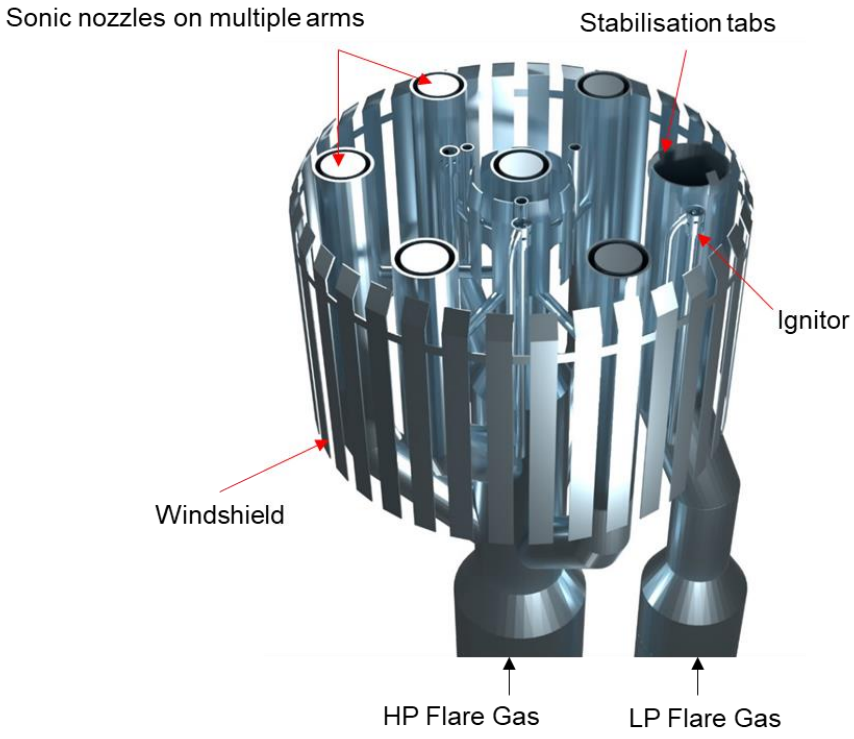

Fig. 6 An example a flare metering installation.

The purpose of the CFD modelling of the flare tip was to assess the combustion efficiency (CE) and destruction and removal efficiency (DRE) of the flares to understand the quantity of hydrocarbon emissions that are released into the atmosphere.

The size of a flare tip system is typically governed by the maximum flow condition such as an emergency shutdown. The flare is also specified to operate at a minimum purge flow rate to maintain a constant flame. Furthermore, these flares can operate in quiescent atmospheres, where the exit velocity from the flare is much higher than any cross wind, as well as when the velocity of the crosswind is comparable or higher than the flare gas exit velocity [3]. Improperly operated flares or exposure to different weather patterns such as crosswinds can influence the flame stability, CE, DRE, and emissions which ultimately result in unburnt hydrocarbons being released into the atmosphere.

Measurement of the combustion efficiency in the field can prove difficult as this requires knowledge of the combustion chemical species and mass fluxes surrounding the flare. This is impractical as the measured chemical species become diluted in the surrounding atmosphere, the flares can be unsteady due to external wind conditions and the sampling locations are difficult to physically access due to the flame and stack height.

Computational Fluid Dynamics (CFD) coupled with detailed combustion chemistry mechanisms can provide information on the combustion efficiency and pollutant emissions of flare tips. This is also a tool that can allow for controlled operational sensitivities such as the effect of fuel composition, flow rate, crosswind, or geometrical changes such as flare tip design. This approach has complimented experimental testing to help understand combustion problems [4, 5, 6, 7].

Based on a series of flare performance studies that were conducted in the early 1980s, a combustion efficiency above 98 % could be achieved when operated under conditions representative of good industrial operating practices [8, 9]. The study focused on air and steam-assisted flares over a wide range of continuous low flow industrial applications and excluded abnormal flaring conditions such as large hydrocarbon releases during process upsets, start-ups and shutdowns. It is the general consensus that most flares operate above 98 % CE and DRE, however, the reports only considered limited fuel inputs (e.g. natural gas with propylene or propane).

The flare tip design is non-assisted and within the current project, NEL have analysed 59 flare tips and 53 were non-assisted. However, the majority of the information on flaring to develop emissions factors in the US has been based on mainly steam or air assisted flares [10]. An EPA review of flaring data and tip design indicated that most of the data was focused on refinery flares where 80 % of the flares are steam assisted, 10 % air assisted and 10 % unassisted [10]. Therefore, the assumption that a value of 98 % is also appropiate to non-assisted offshore flares is questionable because the majorty of data used to support this number are on assisted flares.

Flare tips should be designed to operate with a stable flame over the full operating range for all of the anticipated wind speeds and poor operation can lead to tip damage due to high temperatures, corrosion and flame attachment. When using a flammable purge gas, the flow rate of gas should be high enough to maintain a small visible flame at the tip and prevent burnback. If the flow is too low, the flame might dissappear, may start to smoke, cause overheating and damage to the tip and increase the risk of potential flashback. Low combustion efficiencies can also occur when the flame is unstable and this can be a function of the heating value of the gas and the exit velocity [9].

4.1 Definitions

4.1.1 Combustion efficiency

The term 'combustion efficiency' is defined as the percentage of the flare emissions that are completely oxidised to carbon dioxide (CO_2) and is a measure of a flares' performance.

The most complete definition considers the actual mass flow rate of CO_2 produced from the flare against the theoretical maximum amount of CO_2 that can be produced from the available fuel which has undergone complete combustion. This is easily considered in a closed environment application like a combustion chamber or test facility, or in a numerical model such as CFD where a fixed quantity of fuel and oxidiser enter and exit the model.

In a CFD simulation, the combustion efficiency is reported as

$$CE = \frac{\dot{m}_{CO2,outlet}}{\dot{m}_{CO2,theoretical}} \times 100\ (\%) \tag{5}$$

where the predicted mass flow rate of CO_2 from the outlet of the model, is given by $\dot{m}_{CO2,outlet}$ and the theoretical quantity of CO_2 that can be produced is given by $\dot{m}_{CO2,theoretical}$.
It should be noted that combustion efficiency is defined as complete combustion but is not directly relatable to destruction of hydrocarbons as incomplete combustion can cause intermediate species such as carbon monoxide and other carbon species.

4.1.2 Destruction and removal efficiency

The destruction and removal efficiency (DRE) is the mass percentage of species i that is destroyed relative to the quantity of species i that enters the flare. In this report the destruction and removal efficiency is reported as [11]:

$$DRE = \left(1 - \frac{Y_{plume}}{Y_{in}}\right) \times 100 \tag{6}$$

where:

DRE = destruction and removal efficiency (%).
Y_{plume} = mass flow rate of species X found in the flare plume after combustion has ceased.
Y_{in} = mass flow rate of species X found in the vent gas entering the flare.

As with the combustion efficiency calculations, this is easily considered in a closed environment application such as CFD where a fixed quantity of fuel and oxidiser enter and exit the model.

4.1.3 Emissions rate

The emissions of a chemical species i is reported as the ratio of species i at the outlet of the CFD simulation over the mass flow rate of the fuel at the inlet to give the emission as g/kg_{fuel}, defined as:

$$E_i = \frac{\text{Mass flow rate of species i at the outlet (g/s)}}{\text{Mass flow rate of fuel at the inlet (kg/s)}} \quad (7)$$

4.2 CFD approach

4.2.1 Geometry and mesh

The 3D model of the flare tip case is created from either 3D CAD or engineering drawings. The flare tip is then placed within a fluid region which represents the atmosphere and oriented appropiate to the desired wind direction. The boundaries of the atmospheric domain are chosen to be sufficiently far from the flare to avoid any interference of ill-posed boundary conditions. An example of the 3D fluid region is shown in Figure 7.

The partial differential equations that govern fluid flow and heat transfer are highly non-linear and must be solved numerically. Therefore, in order, to analyse fluid flows, flow domains are split into smaller sub domains. The governing equations are then numerically discretised and solved inside each of these subdomains. The subdomains are often called finite volumes, elements or cells, and the collection of all elements is called a mesh. A high quality Poly-Hexcore mesh was used for the simulations however due to the nature of the flame, the lower wind speeds resulted in a vertical flame whereas the higher wind speeds result in a more horizontal flame. The mesh was therefore refined to cover the entire flame region and mesh sizes around 50 – 150 million cells are typically used depending on the complexity of the flare tip. The meshing approach allows high quality surface meshes to be created to resolve the complexity of the flare gas tip and sufficient refinement in the surrounding flame but fewer cells away from the combustion zone to reduce computational costs without compromising on accuracy.

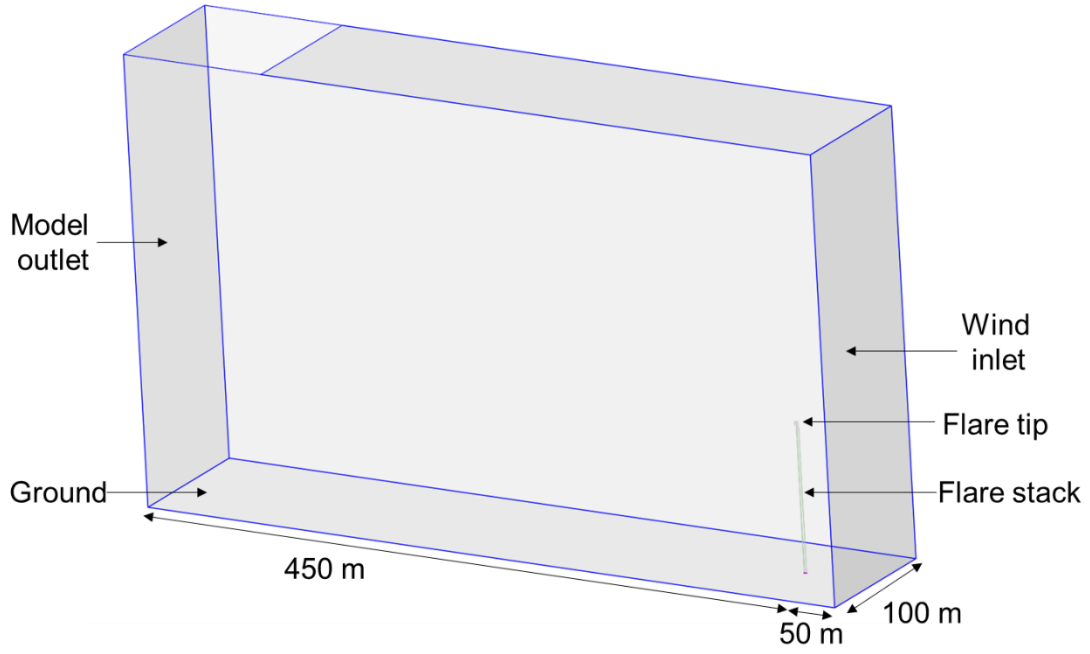

Fig. 7 An example of the fluid region within the domain.

4.2.2 Models

The choice of turbulence model, combustion physics and chemistry play an important role in the prediction of the combustion efficiency and destruction and removal efficiency. The models used were chosen based on comparisons with experimental data and an example case is described in Section 4.3.

4.2.2.1 Turbulence

The aim of the simulation of the flare tip is to provide a time-averaged solution and this is obtained using steady-state methods if the flame is relatively stable. Due to the wide range in length and timescales in the mixing and reacting processes in industrial flames, this is sometimes not possible to achieve and is case dependent.

Typically, a steady-state simulation using the Generalised k-ω (GEKO) turbulence model with parameters adjusted for adequately capturing jet flows that are experienced in flame tips is used [12].

4.2.2.2 Combustion physics and turbulence chemistry interaction

The combustion process was modelled using the partially premixed combustion model with a diffusion flamelet generated manifold. This combines the concepts of steady flamelet combustion modelling which is widely used in modelling diffusion flames and premixed combustion modelling used for modelling the flame front of premixed flame.

The models also account for elements of detailed combustion chemistry that aid the prediction of pollutants, flame lift off and quenching. This also allows the solution of slower forming intermediate species such as carbon monoxide (CO) or nitric oxides (NOx) to be modelled separately, providing more representative values.

The justification for using the partially premixed model is the ability to decouple the chemistry and flow field calculation allowing for an economic investigation of turbulent flames with detailed chemistry.

A detailed combustion mechanism was used for the chemical mechanism and reaction database which is suitable for natural gas and heavier hydrocarbons combustion [13]. The interaction of the turbulence and chemistry was accounted for by a probability density function (PDF). The PDF is a statistical distribution of a randomly fluctuating variable at a fixed point in space sampled over an infinite amount of time.

Using a detailed gas compositional analysis from the flare gas and the ambient conditions, the mechanism can be reduced into a look-up table. The table is a function of the mixture fraction (a normalised variable based on a ratio of a combustible mixture and an oxidser stream), mixture fraction variance, progress variable (a normalised variable related to whether the mixture is ‘burnt’ or ‘unburnt’) and progress variable variance.

4.2.2.3 Boundary condition

The flare flow rate was driven by a mass flow inlet at each of the flares at a given line temperature and pressure. The fluid properties such as the density, viscosity and heat loss / gain are then derived from the look-up table.

4.3 CFD validation

There is a limited amount of CE and DRE data from industrial flare tips which is in part due to the size of the tips and the appropiate measurement strategy. Experimental tests have included small scale laboratory equipment [14, 15, 16] and larger scale testing in wind tunnels [7, 17] or from laser based measurements [18] or extractive measurement sampling techniques [11, 9]. Other techniques such as the use of drones and aerial footage have also been utilised. Each method has its own advantages and disadvantages.

The measurement of flare emission data is diffucult due to the irregular nature and dilution of flare flames due to the ambient conditions such as wind and its direction, effects of high temperatures and radiation on testing equipment, and inaccessibility of the sampling equipment due to the height or location of the flare [7]. In a real world application where the wind dilutes the reactant or product gases, it is difficult to compute the corresponding efficiencies without knowning the composition and mass flux of both the flare gas and wind surrounding the flare. It is therefore very difficult to provide real-time analysis without the use of a model to fully predict or compliment any limited data that may be available. Advances in HPC (high performance computing) technology have allowed CFD to be a viable approach to examine different scenerios that can allow for continuous CE and DRE values for specific tips. However, either approach requires validation of the model.

Experimental data from the flaring testing facility (FTF) operated by CAMNET was used for the CFD model validation [7]. This was used because the geometry of the "flare" and the wind tunnel was relatively simple and non-proprietary so could be easily replicated from publically available documents.

4.3.1 Experimental and CFD set-up

A schematic of the facility is shown in Figure 8 which consists of a 4 inch carbon steel flare pipe of 1 m height in a wind tunnel with a working section that is 1.2 m wide, 8.2 m long and 1.8 m in height. The fuel and ambient air gas composition and flow rates are shown in Table 2. The fuel flow rate was fixed at 20 kg/h at 300 K and the cross wind velocity was between 3 – 12 m/s at 287 K.

The gas was sampled from a 0.46 m sintered metal tube placed at the centreline of the stack and passed to a set of analysers that measuremed O_2, CH_4, CO and CO_2. The concentration of the ambient air was also measured and contained 350 - 400 ppm of CO_2.

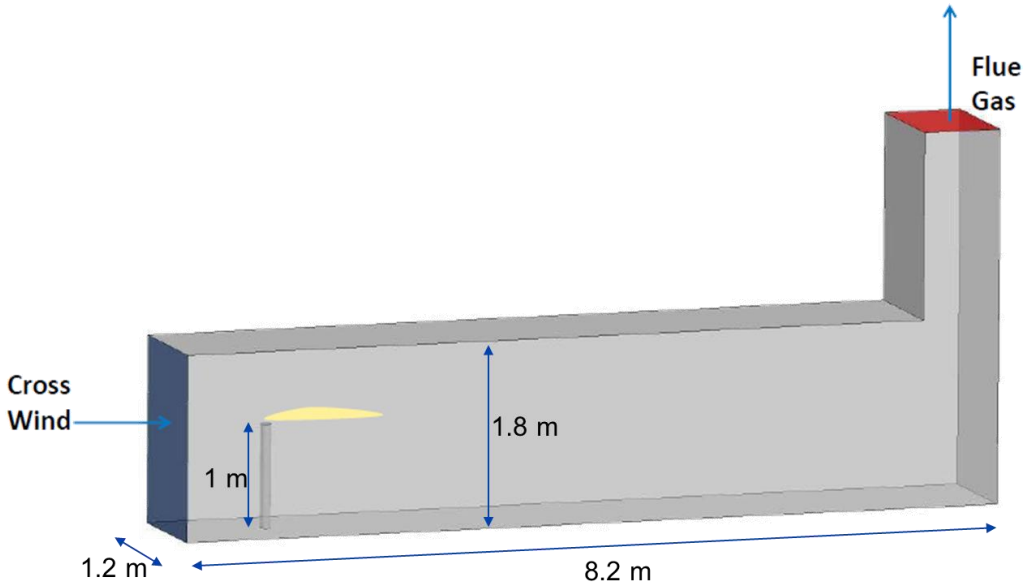

Fig. 8 An example of the fluid region within the domain.

Table 2 – Gas and air composition

	Gas composition (vol, %)						
	N_2	CO_2	CH_4	C_2H_6	C_3H_8	C_4H_{10}	O_2
Fuel gas	1.80	0.62	95.33	2.10	0.13	0.02	0.00
Air	79.07	0.04	0.00	0.00	0.00	0.00	20.89

A high quality poly-hexcore mesh was used for the simulations of around 8 million cells. The simulations were performed in steady state using the turbulence model and combustion chemistry approach stated in Section 4.2.

4.3.2 Results

The simulations were performed at four different wind tunnel speeds of 3, 6, 9 and 12 m/s. The contours of temperature are shown in Figure 9 which show as the wind

speed increases the flame becomes stretched and is further cooled. The CFD results of combustion efficiency, CO_2, O_2 and CH_4 concentration are shown against the measurements in Figure 10 and agree well with the experimental data.

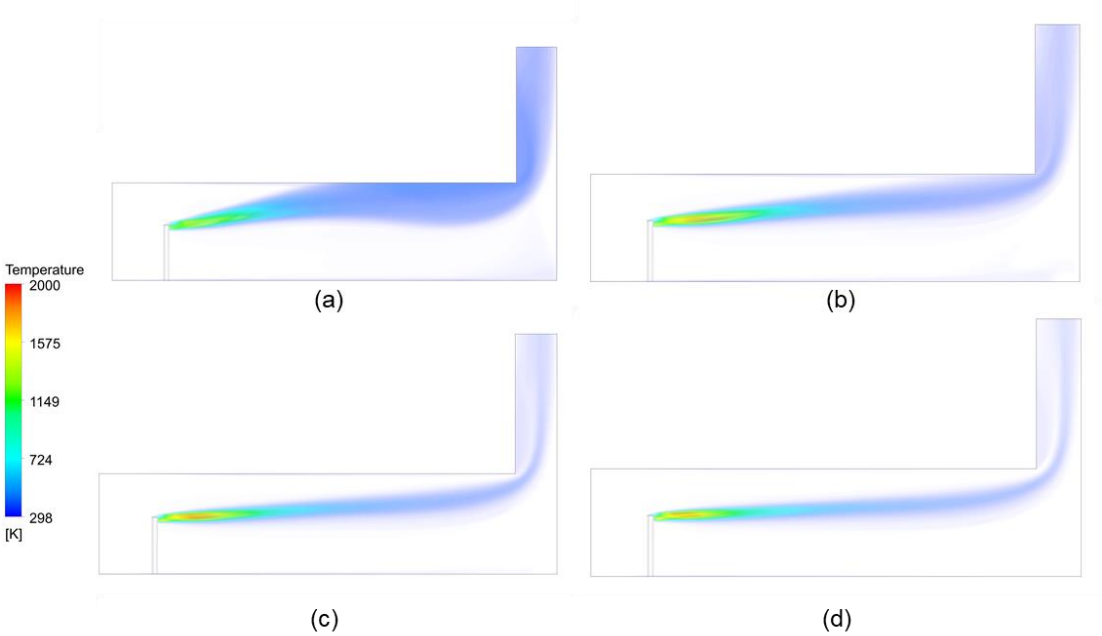

Fig. 9 CFD gas temperature contours for (a) 3 m/s, (b) 6 m/s, (c) 9 m/s and (d) 12 m/s.

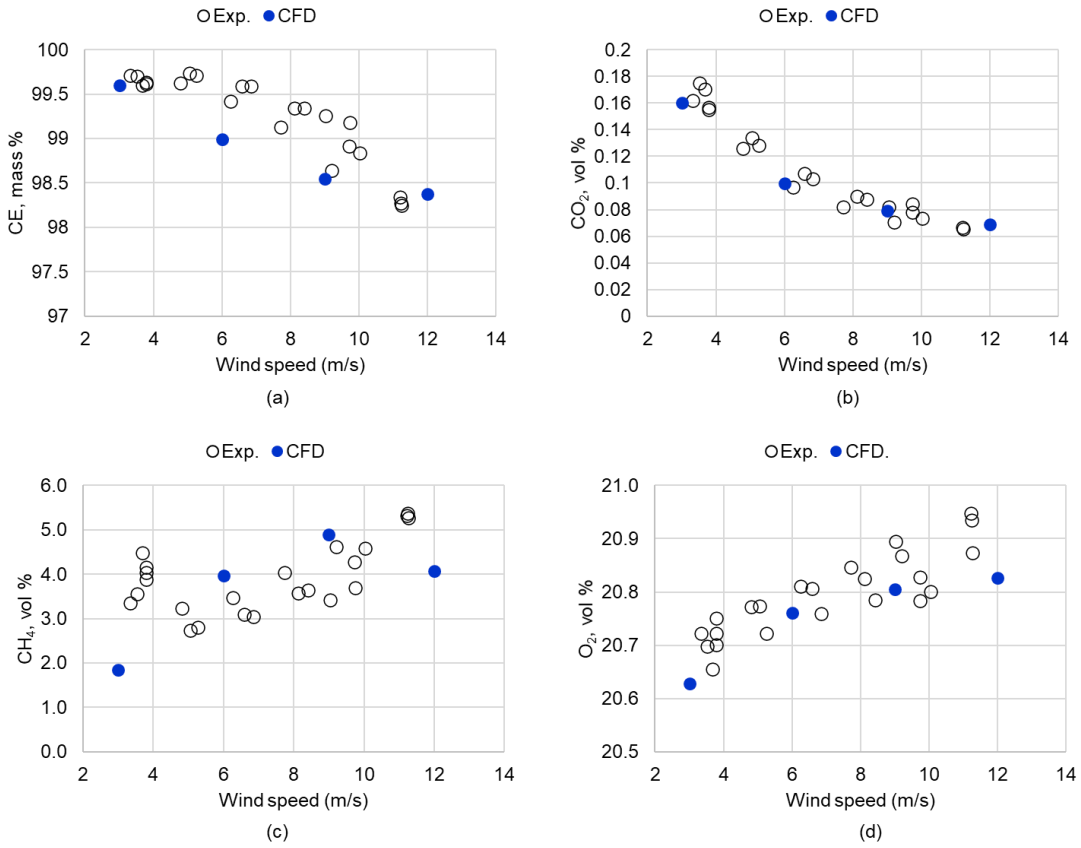

Fig. 10 CFD results plotted against the experimental data set showing combustion efficiency, CO_2, CH_4 and O_2 concentrations.

4.4 Results and discussion

The model described in Section 4.2 and validated against experimental data in Section 4.3 was then used on bp's flare tips to generate a prediction of CE and DRE values. In addition, the CFD simulations have also given an insight into potential operational issues such as air ingress and stabilisation of the flame on the flare body and its components. Sustained operation could lead to thermal damage of the tip over time and reduce the lifetime of the tip itself. An example of a typical output is shown in Figures 11 and 12 which shows a cross section of temperature and oxygen on an HP and LP flare tip for different wind conditions. At higher wind speeds, there is a clear impact on both the flame shape and CE and DRE values.

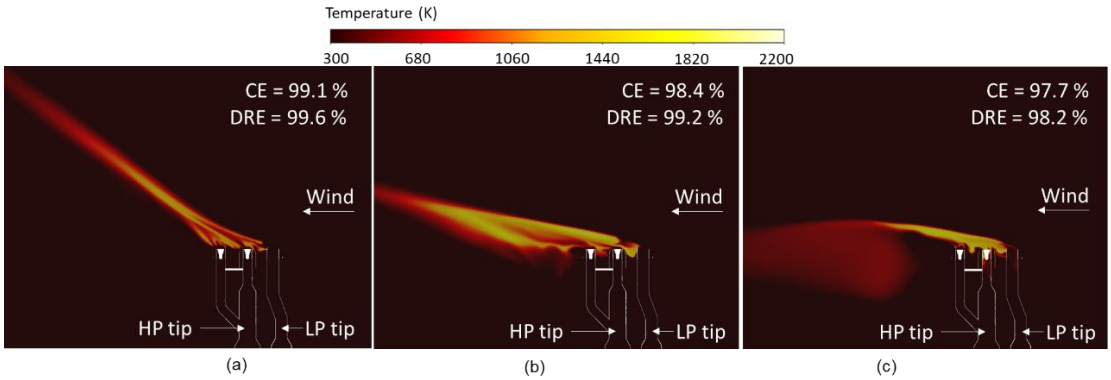

Fig. 11 Gas temperature cross-sectional contours of an HP and LP flare tip for (a) 2.6 m/s, (b) 8.5 m/s and (c) 17.1 m/s showing the CE and DRE values.

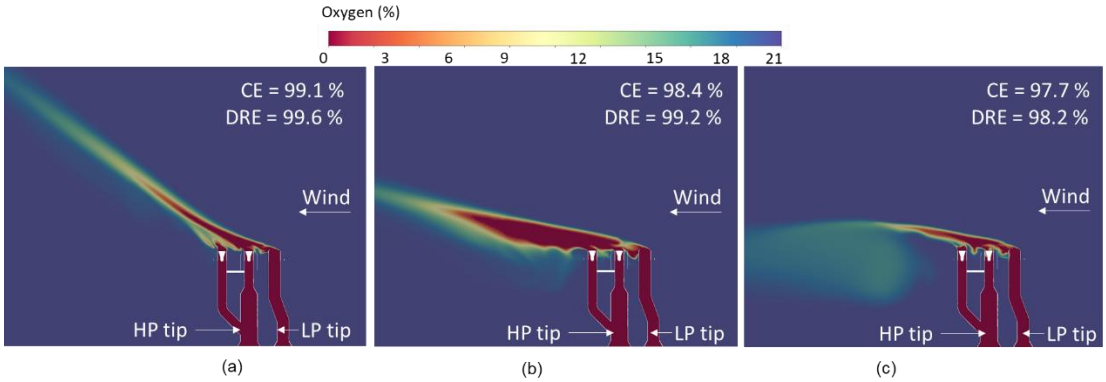

Fig. 12 Oxygen concentration cross-sectional contours of an HP and LP flare tip for (a) 2.6 m/s, (b) 8.5 m/s and (c) 17.1 m/s showing the CE and DRE values.

A further example is shown in Figure 13 where drone footage noticed deformation of the wind shield during an inspection in 2021. The CFD analysis was conducted and reported in 2020 and also highlighted this issue. These observations are fairly common from the CFD analysis and tend to happen at higher wind speeds and lower flare gas flow rates. Air ingress conditions are typically limited to multiple slot or nozzle flare tips at low flare gas / purge flow rates and high wind speeds where an imbalance of pressure within the tip can result in an uneven distribution of flare gas exiting each arm.

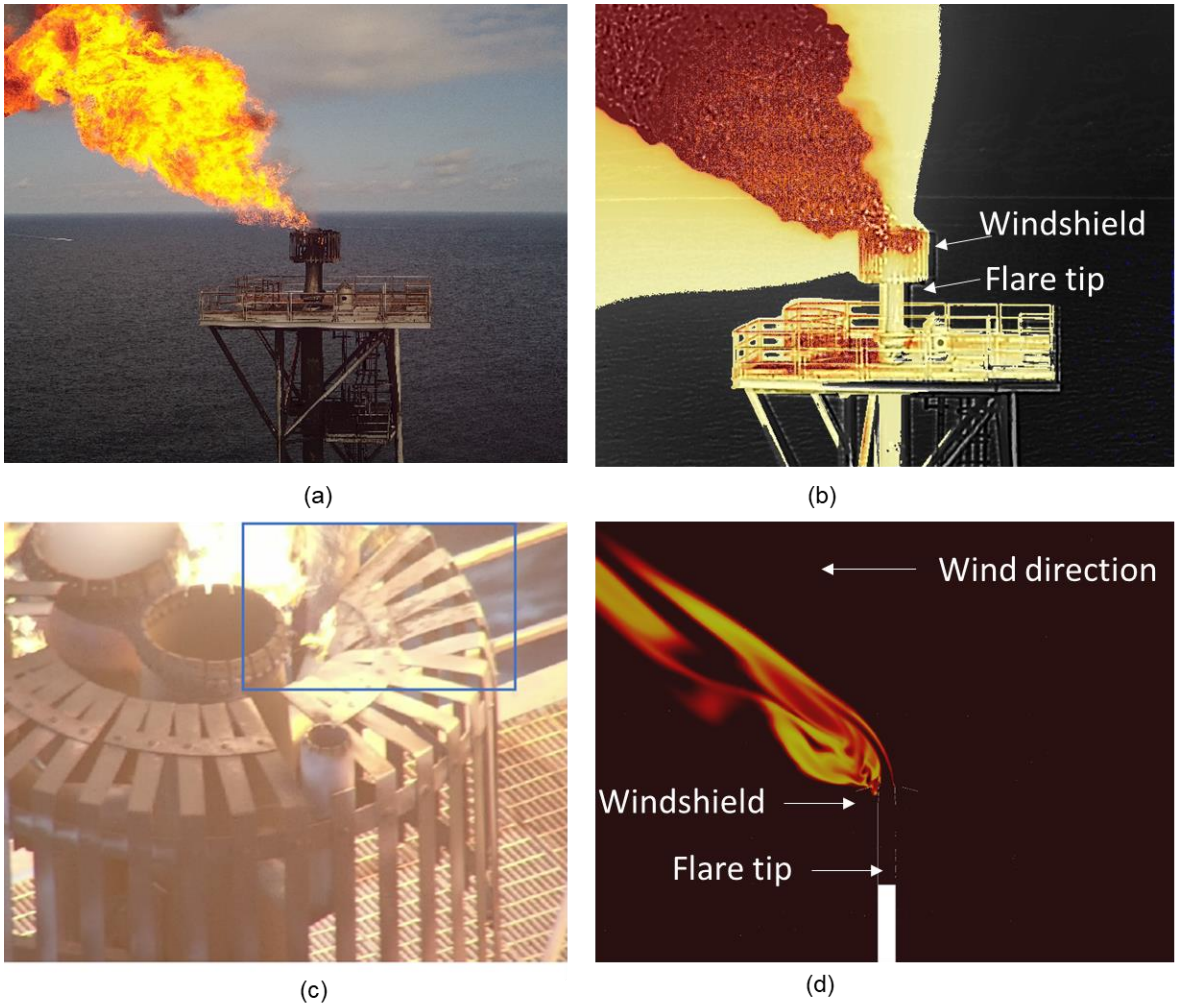

Fig. 13 Images showing (a) drone footage of a flare tip, (b) thermal imaging images, (c) windshield damage highlighted by the blue box and (d) CFD prediction through a cross-section of the flare tip.

Experimental research into the effect of wind on the performance of a flare is limited. The wind can have a large impact on the combustion efficiency of the flare as it can encourage both the quenching of the turbulent eddies of the flame but can also push the flame in the direction of the wind and stabilise behind the flare tip [19]. A dimensionless parameter known as the momemtum flux ratio can be used to provide a ratio of the crosswind velocity and nozzle exit velocity of the flare gas tip [11]. The momentum flux ratio, R, is defined as:

$$R = \frac{\rho_f V_f^2}{\rho_w V_w^2} \tag{8}$$

where ρ_f, ρ_w and V_f, V_w are the density and velocities at the exit of the flare tip and the wind respectively.

The momentum flux ratio is plotted against the CE and DRE of all of the simulations conducted to date in Figure 14. As can be seen from the data, a MFR above 10 would typically result in good operation and CE and DRE values above 98 %. In this condition, the flame is near vertical and the wind has minimal impact on its operation. Flame stabilisation issues typically occur below a value of 5 as the wind pushes the flame over into the direction of the wind. High temperature regions can occur near the windsheld and the flame can become attached on to the flare body. Below 0.1, there is usually insufficient momemtum to completely purge the flare gas from the flare tip and some recirculation of air and flare gas may occur in the tip body. It is important to note that API RP 521 considers that the majority of hydrocarbon mixtures are considered safe and non-flammable with 6% or less oxygen in the mixture at up to 25 ft inside the tip from its exit, except where large quantities of hydrogen are present. It should be noted that the results presented in Figure 14, labelled as "flare gas too low" consider the situation where any level of air ingress has occurred.

Authors in the literature have suggested the MFR is a poor correlative parameter for the effect of wind speed on the combustion efficiency of flare flames [19]. Generally, the experimental evidence that has been gathered suggests that flares operating well above the limit of their stability generally have combustion efficiencies greater than 98 % and combustion efficiencies may be low if operating near their stabilitiy limit [9]. The stabilility of a flame is a balance of the flame speed and imposed velocity and is influenced by its shape, pilot ignitors, ambient wind or additional air or steam. Relationships have been investigated with good correlations between flare gas exit velocity and gas heating value [17, 11]. It should be noted that flare velocity regulations 40 CFR 60.18 stipulate a minimum net heating value of 300 Btu/scf for steam assisted or air-assisted flares or 200 Btu/scf for non-assisted flares and most of the simulations shown in Figure 14 were significantly above this value.

In summary, the results to date demonstrate that a correlation for CE and DRE with flare gas velocity, heating value, ambient conditions and tip design is difficult to define. Therefore, using detailed combustion models coupled with CFD allows bp to have a representative idea of the performance of each of their flares in current and in future scenerios.

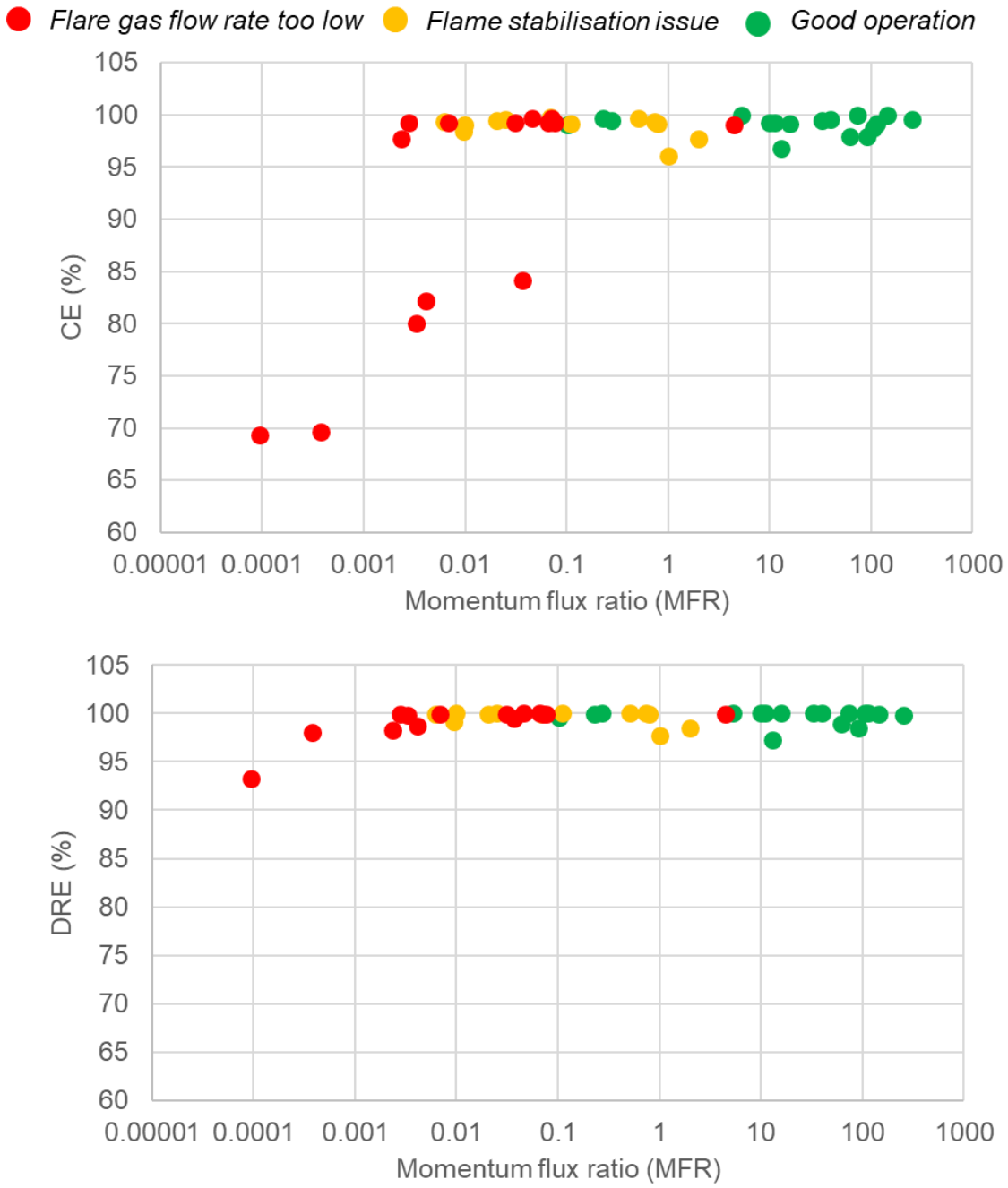

Fig. 14 Momentum flux ratio plotted against CE and DRE. Colours highlight if good operation (green), flame stabilisation on the tip body or windshield (yellow) and if there is a possibility that the flare gas flow rate is too low (red).

5 CONCLUSIONS

This paper demonstrates the use of and highlights the merits of CFD performed by TÜV SÜD National Engineering Laboratory (NEL) on bp's global production flare and vent systems, with the aim of understanding, verifying and ultimately reducing bp's overall methane intensity in a safe and efficient manner from all of bp's global production assets. This is part of bp's Aim 4 plans in support of delivering its net zero ambition.

Accurate flare and vent gas metering is important to report the correct quantities of flare gas flowing to the vents or flares. This is important in meeting regulatory requirements but also for understanding efficient operation of the flare tip. CFD modelling has been used to construct 3D models of the flare metering system and flare tip to provide information on metering errors related to installation effects and information related to the efficiency and overall operation of the flare tip.

Where possible, the CFD models have been verified against experimental data or incorporated into an uncertainty analysis to ultimately provide confidence in the predictions. This paper demonstrates this approach as a valuable method to increase flaring and venting knowledge and help significantly reduce the impact on the environment from flaring and venting.

6 REFERENCES

[1] I. E. Agency, "World Energy Outlook 2021," IEA, December 2021.

[2] T. NEL, "Good Practice Guide: Flare Gas Measurement Using Ultrasonic Transit-Time Flow Meters," TUV NEL, Glasgow.

[3] A. A. Aboje, "Numerical and Experimental Study of Methane and Propane Flames in relation to Gas Flaring," PhD Thesis, University of Leeds, Leeds, 2015.

[4] M. C. B. Dolinsky, "Basic Engineering Design of Flares on Oil Platforms using Computational Fluid Dynamics," in *ESSS Conference & ANSYS users meeting*, May 19-21, 2014.

[5] M. Henneke, "CFD prediction of visible flame length for pressure-assisted flares," in *AFRC 2014 Industrial Combustion Symposium*, Houston, Texas, Sept 7-10, 2014.

[6] A. Jatale, "Modelling CO and estimating combustion efficiency with flamelet-generated manifolds in flare," in *AFRC 2014 Industrial Combustion Symposium*, Houston, Texas, Sept7-10, 2014.

[7] A. Jatale, P. Smith, J. N. Thornock and S. T. Smith, "A validation of flare combustion efficiency simulations," in *American Flare Research Committee 2012 Industrial Combustion*, Salt Lake City, September 2012.

[8] B. A. Tichenor, "Flare Efficiency Study," US Environmental Protection Agency, Washington, 1983.

[9] J. H. Pohl and B. A. Tichenor, "Flare Efficiency - the influence of flare head design and gas composition," Air and Energy Engineering Research Laboratory, Accession Number PB85225068, 1985.

[10] "EPA Review of Available Documents and Rationale in Support of Final Emissions Factors and Negative Determinations for Flares, Tanks and

Wastewater Treatment Systems," U.S. Environmental Protection Agency, North Carolina, April 2015.

[11] D. T. Allen and V. M. Torres, "TCEQ 2010 Flare Study Final Report," University of Texas, Austin, 2011.

[12] F. R. Menter and R. Lechner, "Best Practice: Generalized k-w two equation turbulence model in ANSYS CFD (GEKO). Version 1.00. Technical Report," ANSYS, January 2019.

[13] "CRECK Detailed Combustion Mechanism C1-C16 HT mechanism (version 2003)," [Online]. Available: http://creckmodeling.chem.polimi.it/. [Accessed March 2020].

[14] R. F. Huang, "Characteristic Flow Modes of Wake-Stabilized Jet Flames in a Transverse Air Stream," *Combustion and Flame,* vol. 117, pp. 59-77, 1999.

[15] R. F. Huang and J. M. Chang, "The Stability and Visualized Flame and Flow Structures of a Combusting Jet in Cross Flow," *Combustion and Flame ,* vol. 98, pp. 267-278, 1994.

[16] R. F. Huang and M. J. Yang, "Thermal and Concentration Fields of Burner-Attached Jet flames in Cross Flow," *Combustion and Flame,* vol. 105, pp. 211-224, 1996.

[17] P. Gogolek, "Methane emission factors for biogas flares," *Journal of the International Flame Research Foundation,* no. Article Number 201203, 2012.

[18] R. A. Robinson, A. S. Andrews, T. D. Gardiner, I. J. Uprichard and P. T. Woods, "Differential Absorption Lidar Measurements of VOC Emissions from Wytch Farm Crude Oil Gathering Station," National Physical Laboratory, Teddington, 1998.

[19] J. H. Pohl, N. R. Soelberg and J. A. Seebold, "Combustion Efficiency of Flares and the effect of wind," in *14th AFRC Symposium*, Houston, 2014.

[20] I. O. f. Standardization, "ISO 16911-2:2013 Stationary source emissions — Manual and automatic determination of velocity and volume flow rate in ducts — Part 2: Automated measuring systems," International Organization for Standardization, 2013.

7 NOTATION

CAD Computer Aided Drawing
CE Combustion Efficiency
CFD Computational Fluid Dynamics
DRE Destruction and removal efficiency
EPA Environmental Protection Agency
ETS European Trading Scheme
FTF Flaring test facility
GEKO Generalised k-ω
HP High pressure
HPC High Performance Computing
LP Low pressure
MFR Momentum flux ratio
NEL TÜV SÜD National Engineering Laboratory
PDF Probability density function
UFM Ultrasonic Meter

E_i emission rate of chemical species i (kg/s)

L_{path}	path length between two transducers (m)
T_{ij}	transit time from transducer i to transducer j (s)
V_f	average flare gas velocity at the exit of the flare tip (m/s)
V_{path}	gas velocity of an individual meter path (m/s)
V_w	average wind velocity at the flare tip (m/s)
Y_i	mass flow rate of chemical species i (kg/s)
D	pipe diameter (m)
Q	volumetric flow rate (m3/s)
R	Momentum flux ratio
Re	Reynolds number (dimensionless)
X	mean
Z	lateral distance along the pipe axis (m)
k	k-factor or correction factor (dimensionless)
n	number of sensitivities
μ	dynamic viscosity (kg/m-s)
ρ	density (kg/m3)